ELSEVIER

Thermochimica Acta 377 (2001) 131–140

thermochimica acta

www.elsevier.com/locate/tca

An AC calorimeter for the study of solid–solid phase transitions

A. Fraile-Rodríguez[a,*], I. Ruiz-Larrea[b], A. López-Echarri[a], M.J. Tello[a]

[a]*Departamento de Física de la Materia Condensada, Facultad de Ciencias, Universidad del País Vasco, Apdo. 644, 48080 Bilbao, Spain*
[b]*Departamento de Física Aplicada II, Facultad de Ciencias, Universidad del País Vasco, Apdo. 644, 48080 Bilbao, Spain*

Received 6 July 2000; received in revised form 28 January 2001; accepted 2 February 2001

Abstract

An AC calorimeter ranging from 4.2 to 400 K has been built and optimized in our laboratory for the study of solid–solid phase transitions. Only a small amount of sample is required (with typical dimensions of $(2-6)\,\text{mm} \times (2-4)\,\text{mm} \times (0.2-0.5)\,\text{mm}$ and mass around 1–25 mg) and different types of solids such as insulator crystals or metal samples can be studied. Small-diameter thermocouples (25 μm) are used as temperature sensors and also as sample support. This system can be operated discontinuously with temperature jumps as small as 0.025 K or by continuous heating or cooling with scanning rates from 0.06 up to 6 K/min. Both procedures are governed by an automatic control program and data acquisition which provides very low dispersion of the C_p points (0.1%). The whole experimental set up was tested by new measurements of the triglycine sulphate (TGS) specific heat. Finally, the ferroelectric phase transition in the TGS is studied within the frame of the Landau theory. With this model, the specific heat is correctly described down to 15°C below the transition temperature leading to accurate calculations of the phase transition thermodynamic functions.

Keywords: AC calorimetry; Phase transitions

1. Introduction

At present, several experimental techniques for calorimetric studies of solid–solid phase transitions are commonly used. Among them, adiabatic calorimetry is considered one of the most accurate calorimetric methods but its accuracy drops when a high density of specific heat points in short temperature ranges are needed. In this case, very small temperature increments are required and, even if a Pt-resistance thermometer is used, the temperature unaccuracy increases the dispersion of the C_p points [1]. In addition, samples of a rather large mass (more than 100 mg) are usually required.

All the shortcomings previously mentioned are not present in the so-called AC calorimetry which has been developed in the last 30 years ([2], and references therein). With the use of this technique, only a small quantity of sample is needed (masses of order 1–25 mg and typical dimensions of about $2\,\text{mm} \times 2\,\text{mm} \times (0.1-0.3)\,\text{mm}$). The AC methods show a low data dispersion (typically 0.1% in C_p) and are therefore very successful in measuring structural phase transitions when the associated specific heat anomaly is very low. AC calorimetry has some other advantages for the study of phase transitions in solids. Measurements can be performed in a wide range of temperatures, without the strict adiabatic conditions (see, for instance, [3–5]). On the other hand, the use

* Corresponding author. Tel.: +34-94-601-5340; fax: +34-94-464-8500.
E-mail address: wmbfrrom@lg.ehu.es (A. Fraile-Rodríguez).

0040-6031/01/$ – see front matter
PII: S0040-6031(01)00548-2

of very small temperature steps becomes specially important in the precise determination of the specific heat in the close vicinity of the critical temperature. Finally, hysteresis effects can be studied since cooling and heating measurements can be easily performed.

One of the most important disadvantages of this technique is the experimental difficulty to obtain absolute specific heat values. Moreover, it is not possible to measure the latent heat present in first-order phase transitions. In some works, the behaviour of the phase shift between the heating power and the thermal response of the system is claimed to be related with the character of the transition [6]. Indeed, indirect measurements of the latent heat have been studied by several groups [7–9].

In this work, we present the experimental installation of an AC calorimeter. The various measurement procedures and the automatic control and data acquisition are also described. The characteristics and performance of the system was tested by means of a sample of a well-known ferroelectric crystal such as the triglycine sulphate (TGS). Finally, the obtained specific heat values are briefly discussed within the frame of the Landau theory.

2. AC calorimetry

Although the first reported measurement by AC calorimetry was carried out in 1910 by Corbino [10], it was after the work of Sullivan and Seidel [11] and Handler et al. [12], when measurements were made in a wider temperature range favouring the development of this new technique.

The principle of AC calorimetry is to heat the sample periodically and detect the amplitude of the small temperature oscillations, ΔT_{ac}, around the mean temperature of the thermal reservoir to which the sample is thermally anchored. As we will see later, the specific heat of the sample can be obtained by measuring the amplitude of this temperature oscillation, which is found to be proportional to the inverse of the sample specific heat.

The dynamic behaviour of the system with oscillatory heat input involves two characteristic time constants: τ_s, which is the relaxation time associated to the thermal coupling among the sample, the thermal links and the thermal bath, and τ_{int}, the characteristic time for the sample to reach the internal thermal equilibrium, depending on the sample thermal diffusivity. By means of the heat diffusion equations and with the use of the principle of energy conservation, Sullivan and Seidel [11] have obtained the amplitude and phase shift of the temperature oscillation for a slab-shaped sample. The general solution for the sample temperature has two different terms. A constant DC component above the thermal bath temperature:

$$\Delta T_{dc} = \frac{P_0 d}{2AK_b} \tag{1}$$

where P_0 is the signal amplitude at the frequency f of the power supplied on the upper surface of the sample, A being the area of the sample, d the distance between sample and the thermal bath and K_b the thermal conductivity of the exchange gas. The second term is an oscillatory AC component whose amplitude is given by

$$\Delta T_{ac} = \frac{P_0}{\omega C_s}\left(1 + \frac{1}{\omega^2\tau_s^2} + \omega^2\tau_{int}^2\right)^{-1/2}, \quad \text{where } \omega = 2\pi f \tag{2}$$

If $\tau_{int} \ll \tau_s$ it is possible to find a frequency f for which the associated terms in (2) can be neglected. Under these conditions, the observed ΔT_{ac} temperature rise is inversely proportional to the heat capacity of the sample, C_s. For this purpose, the chopping frequency f should be higher than $1/2\pi\tau_s$ in order to prevent the AC component of the heat dissipation from the sample. On the other hand, a thermocouple attached to the sample mainly detects the temperature oscillations within a circle of radius equal to the thermal length:

$$l_t = \left(\frac{D}{\pi f}\right)^{1/2} \tag{3}$$

where D is the thermal diffusivity of the sample [11]. Therefore, the upper limit of the frequency must be chosen in such a way that the thickness of the sample L is smaller than the thermal length in the sample: $(D/\pi f)^{1/2} \gg L$. In these conditions, the heat capacity of the sample and the phase shift α values become

$$C_s = \frac{P_0}{2\pi f \Delta T_{ac}}, \quad \text{with } \alpha = \frac{\pi}{2} \tag{4}$$

3. Calorimetric set up and experimental procedures

3.1. Cryostat

An AC calorimeter has been built and optimized in our laboratory to perform specific heat measurements of solid samples in the temperature range: 4.2–400 K. As shown in Fig. 1, it is constituted by two concentric Dewar vessels which hold the calorimetric system. Depending on the range of temperatures where the measurements are carried out, both vessels can be filled with liquid N_2 and/or liquid He. The calorimetric system is formed by a main chamber which contains the sample and acts as the thermal reservoir (copper block). This ensemble is placed inside a secondary chamber which provides a good thermal isolation. Both chambers can be independently evacuated to reduce the thermal contact between the sample and the copper block or helium gas may be used to fill the chamber to increase the thermal conductivity. Vacuum conditions (up to 10^{-1} Pa) can be achieved by using a rotatory pump.

3.2. Lighting and generation of the periodic heating power

Chopped light from a halogen lamp is used to heat the sample periodically. The power supply of the lamp is current stabilised (HP, System Power Supply, model 6038A). A drift stability of $0.02\% + 2$ mV in voltage and $0.03\% + 3$ mA in intensity can be achieved over an 8 h interval under constant line and load. The modulated light beam from the lamp is focused through a lens on a 10 mm diameter glass bent rod which directly guides the light to the sample. This glass rod is roughened on the nearest surface of the sample in order to make the light beam homogeneous. To increase the light absorption of the sample, the illuminated surface is black-painted.

The lighting system which includes the lamp, lenses and chopper is fixed on an optical bench. The whole ensemble is placed inside a metallic box in order to prevent external influences, such as changes of T, draughts, etc. and guarantees the stability of the light beam.

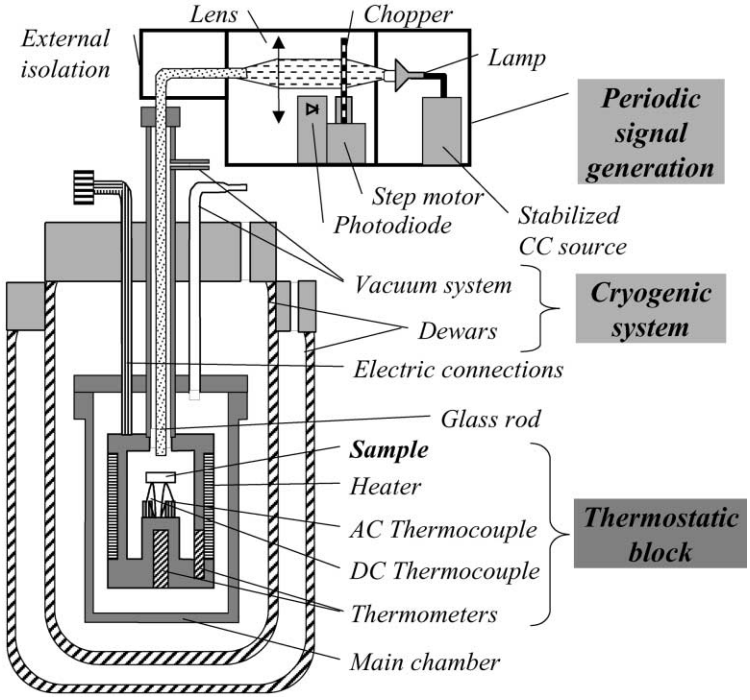

Fig. 1. Diagram of the AC calorimetry set up.

The chopper rotation is driven by a permanent-magnet step-motor. Steps are generated by a drive board which makes the motor rotate with precise steps, 1.8° per step. As frequency generator, two oscillators built-in quartz crystal are used. The high stability of the quartz crystal (20 ppm) assures an extremely stable chopper frequency (<0.1%). The reference frequency signal is delivered by a phototransistor which detects the emitted chopped light.

3.3. Measurement of the temperature of the thermal reservoir, T_B

The heating of the thermal copper block is carried out by a non-inductive winding of constantan wire (0.2 mm thickness, $R = 56\,\Omega$). Varnish (GE 7031) is used as glue and also as a thermal contact enhancer. For the measurement of the temperature of the block, T_B, a platinum resistance thermometer (100 Ω at 273.15 K, Minco Products, model S1059PA5X6), calibrated according to the ITS-90, is used. The platinum thermometer with an absolute accuracy of ±1 mK in the whole range of temperature, is placed at the bottom of the copper block with the leads thermally anchored to. The resistance value, using the 4-wire method, is obtained by means of a 8 1/2 digits multimeter (HP, model 3457A). To regulate the temperature of the system, a PID-temperature controller (Lake Shore Cryotronics, model DRC-93C) is used. This PID provides minimum temperature steps of 25 mK and uses an independent platinum resistance thermometer attached to the copper block to avoid interferences with the most accurate main thermometer.

3.4. Measurement of the thermal oscillations, ΔT_{ac}

In order to attain condition (3), the oscillations of the temperature of the sample should be the same for an area around the AC thermocouple of radius greater than the thermal length. For this purpose, flat plate-shaped samples are needed. Moreover, it is necessary to select a chopper frequency which makes the thermal length greater than the largest dimension of the sample. In our system, typical dimensions of about $(2-6)\,\text{mm} \times (2-4)\,\text{mm} \times (0.2-0.5)\,\text{mm}$ are found to be appropriate.

The choice of the thermocouples is governed by some considerations. The selection of small-diameter wires is very effective in minimizing the addenda. Another restriction is that the length of the leads should be smaller than the thermal length of the thermocouple material [13]. In our experimental set up, two pairs of iron–constantan thermocouples of 25 μm diameter are used as temperature sensors which are used to independently measure the DC and AC temperature components. Their junctions are attached to the rear face of the sample and to the copper block by means of GE 7031 varnish which improves the thermal contact. In the case of metallic samples it is convenient to insulate both thermocouples to avoid the electrical contact between them. The thermocouples wires are directly soldered on 4-pins electrically insulated from the block in such a way that the four leads also serve as sample support. The AC thermocouple signal is delivered to a low-noise transformer (Princeton Applied Research model 190, gain = 100) to match the ∼10 Ω source impedance of the thermocouple to the high input impedance (∼10 MΩ) of the lock-in amplifier (Stanford Research Systems, model SR850). This AC voltage is measured by the lock-in which is driven synchronously with the frequency of the chopped light. Alternatively, this AC voltage can also be driven to an oscilloscope (HP, model 54645A) by using a differential DC chopper amplifier (Ancom, model 15C-3a, gain = 10^6) in order to observe simultaneously both the heating square wave and the thermal response of the sample. The DC voltage of the second thermocouple is measured by the 8 1/2 digits HP multimeter cited above and permits to obtain the temperature difference between the sample and the copper block, ΔT_{dc}. Under these conditions, the temperature of the sample is then given by $T_B + \Delta T_{dc}$. In Fig. 2, a block diagram of the experimental measurement procedure in the AC calorimeter is shown.

3.5. Automation of the system

A program in HP Instrument BASIC language was developed for the automation of the experimental set up. A schematic diagram of the program is shown in Fig. 3. There are two experimental procedures.

In the first procedure, the temperature of the sample is programmed in discontinuous steps. Temperature jumps as small as 0.025 K can be used. After each heating or cooling period, the approach to the thermal equilibrium at the programmed temperatures is

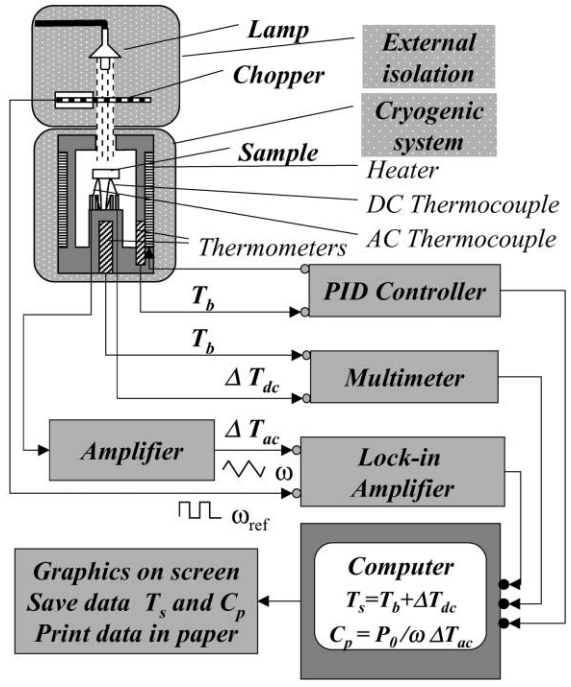

Fig. 2. Block diagram of the experimental equipment for the specific heat measurements.

observed by continuous measurements of the sample temperature ($T_B + \Delta T_{dc}$) until the selected equilibrium criterium is satisfied. Typical drift values are $(dT/dt) \leq 4 \times 10^{-5}$ K/s and $(d^2T/dt^2) \geq 1 \times 10^{-4}$ K/s^2. A number of ΔT_{ac} data are then obtained and the mean value is recorded.

The second procedure allows for continuous heating or cooling of the sample. Scanning rates can be programmed from 0.06 to 6 K/min, approximately. In this case, both the sample temperature and the amplitude of the thermal oscillations are simultaneously recorded. If needed, different computer programs permit to smooth the experimental curve after the scanning is finished.

4. Results

The behaviour and performance of the experimental set up was established by means of a suitable sample of the well-known ferroelectric crystal triglycine sulphate (TGS) which undergoes a second order phase transition at 49°C [14]. The optimization of the experimental parameters such as the light intensity, chopper

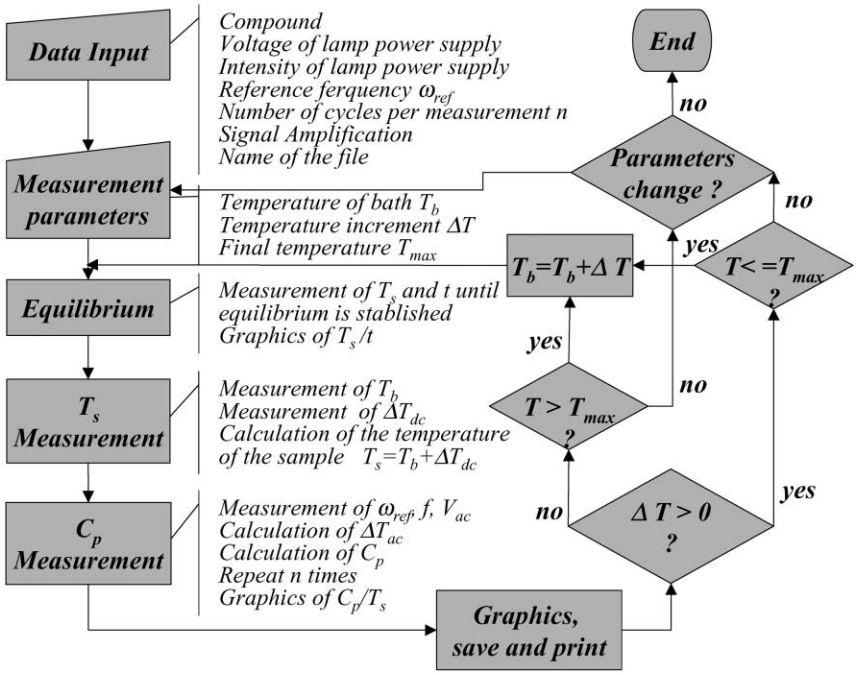

Fig. 3. Schematic diagram of the automatic program for the control and acquisition of the specific heat data.

frequency, the pressure inside the chamber, the AC signal amplification, etc. ... as well as the different measurement procedures were examined in different temperature ranges. The TGS sample was a plate-shaped crystal with dimensions 5.5 mm × 2.0 mm × 0.5 mm and mass $m = 16.95$ mg. Measurements were made at 10^{-1} Pa.

4.1. Relaxation times

As cited above, the requirement $\tau_{int} \ll \tau_s$ is needed for Eq. (4) to be valid. The relaxation times values are not only dependent on the thermal properties of the sample, but also on the detailed experimental conditions. As a consequence, a previous estimation of these values are firmly recommended. Moreover, the thermal relaxation data can be used for a different determination of the sample specific heat [15]. Once the sample is installed in the cryostat, direct measurements of these quantities can be performed in the following way. After the copper block temperature T_B stabilizes, the sample is heated at $t = 0$ by a not chopped beam light of fixed power P for a certain period of time (about 3 min). The temperature rise of the sample as a function of time is recorded. These experimental data are found to fit quite well an exponential relaxation function such as

$$T(t) = T_B + A(1 - e^{-t/\tau_1}) \quad (5)$$

The results of this fit show that A approximates quite well to the experimental value of ΔT_{dc}, which is in agreement with (4) for $t \to \infty$.

A similar result is obtained after suppression of the heating light beam. In this case, the thermal relaxation can be fitted to

$$T(t) = T_B + \Delta T_{dc}\, e^{-t/\tau_1} \quad (6)$$

As a consequence, it is deduced that the thermal relaxation time related to the thermal conductivity of the sample τ_{int} should be very much smaller than τ_1, which is commonly associated to the relaxation time of the sample and its surroundings τ_s [15]. As an example, at $T_B = 300$ K and $P = 48$ W, $\tau_1 \sim 11$ s and $\Delta T_{dc} = 0.13 \pm 0.02$ K. It is also observed that these quantities together with ΔT_{dc} are only slightly temperature dependent.

4.2. Modulated light beam frequency

In order to select a frequency which allows to use the simplified expression (4) for determining the heat capacity, frequency scans at several constant block temperatures and powers must be performed. A plot of ΔT_{ac} as a function of the inverse of the frequency $1/f$ should show a region of proportionality. Moreover, in this frequency region, a $\pi/2$ phase shift between the thermal oscillations and the heating square wave is observed by means of an oscilloscope. Therefore, any frequency value in this interval may be set as the chopper frequency. As it is shown in Fig. 4 the linear dependence for the TGS sample at $T_B = 300$ K lies between 1.0 and 1.6 Hz. The selected frequency values are usually valid for wide temperature ranges.

4.3. Heating power

As it can be observed in (4), even if f and ΔT_{ac} are measured, the specific heat of the sample can only be determined if the actual absorbed power P_0 is known. As it could be expected this task is, if not impossible, extremely difficult. This explains the fact that absolute C_p results are normally out the scope of the AC methods. Only careful calibrations have permitted in some few cases a reasonable approach to the true specific heat values [6]. However, a high stability of the heating power during measurements is required to guarantee the proportionality between C_p and $1/\Delta T_{ac}$. The variation of the beam intensity as a function of time was accomplished by direct observation of the photodiode electric current. A better procedure is to evaluate the stability of the absorbed light in the sample. It is easily performed by recording the thermal AC oscillations as a function of time at constant frequency and temperature (i.e. $C_p = $ constant). Note that under these conditions, $\Delta T_{ac} \propto P_0$ (4). It is observed that, after 12 h working, the stability of the light beam is very high. On the other hand, the decreasing of the intensity due to the ageing of the lamp is slow and long-term. Moreover, the peak-to-peak temperature oscillations of the sample must be smaller than the temperature interval between two measurements, but as high as possible to reduce noise. In the present case, a lamp power of $P = 48$ W was selected and corresponds to $\Delta T_{ac} \sim 3$ mK.

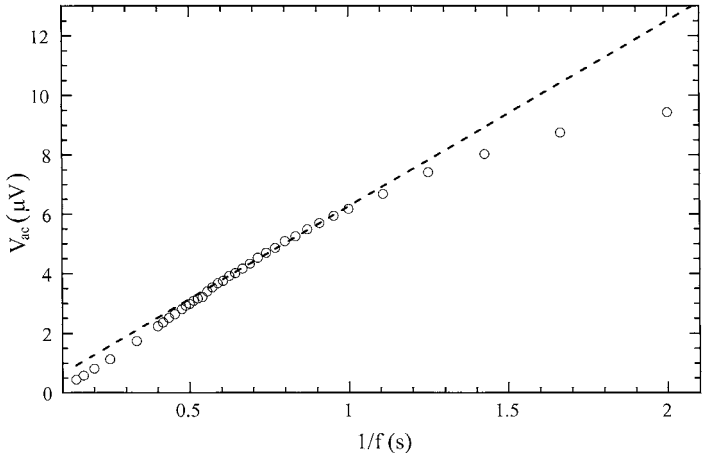

Fig. 4. Frequency scan at constant sample mean temperature. The linear region is in agreement with the direct observation of the $\pi/2$ phase shift of the thermal oscillations. Any frequency value in this interval may be set as the chopper frequency.

5. Discussion

The availability of absolute values of the TGS specific heat obtained by adiabatic calorimetry [16] have permitted us to fit the AC calorimetric results around the phase transition temperature. It has been accomplished by using an unknown constant power of the chopped light as a scaling factor and assuming a linear temperature dependence for the specific heat of the addenda with two adjustable parameters:

$$C_p' = A(C_p + B + CT) \tag{7}$$

where $A = P_0/2\pi f$. The factor C_p represents the absolute specific heat data and C_p' are the experimental AC data. A least square method has been applied to determine the coefficients which lead to the best fit (see below). The addenda contribution in this temperature range is found to be about 3.5% of the total C_p.

The phase transition contribution to the specific heat is usually obtained by means of an appropriate baseline which accounts for the lattice contribution. In this case, this baseline has been determined by a linear extrapolation of the specific heat data at $T > 330$ K. This approximation is usually found not adequate for a precise determination of the total phase transition thermodynamic functions when the associated C_p anomaly extends throughout a wide temperature range. However, it can be considered enough for the study we are performing in a limited range.

As it is well known, the ferroelectric phase transition exhibited by TGS can be described within the frame of the Landau theory for second-order phase transitions. This has been accomplished in the past by means of a free energy expansion as a function of the order parameter (which in this case is the spontaneous polarization) ([17] and references therein). However, a much better fit to the experimental data in a wider temperature range is found if this function is expanded up to the sixth order and the proportionality between the entropy and the squared polarization is used (see below).

$$F = F_0 + \tfrac{1}{2}\alpha P^2 + \tfrac{1}{4}\beta P^4 + \tfrac{1}{6}\gamma P^6 + \cdots \tag{8}$$

As usual, only the second-order coefficient is considered to be temperature-dependent, $\alpha = (4\pi/C)(T - T_0)$, where C is the Curie constant. In this case, the phase transition entropy is obtained by

$$\Delta S = -\left(\frac{\partial F}{\partial T}\right)_{\mathrm{p}} = -\left(\frac{2\pi}{C}\right)P^2 \tag{9}$$

The entropy values can be fitted to the experimental P^2 data [14]. The best fit has been found for $C = 2312$ K. Both quantities are plotted in Fig. 5 showing a good agreement in the range of temperature: $T_0 - T \leq 15$°C.

From the minimization of F with respect to P and taking into account that $C_p = T(\partial S/\partial T)$, the specific

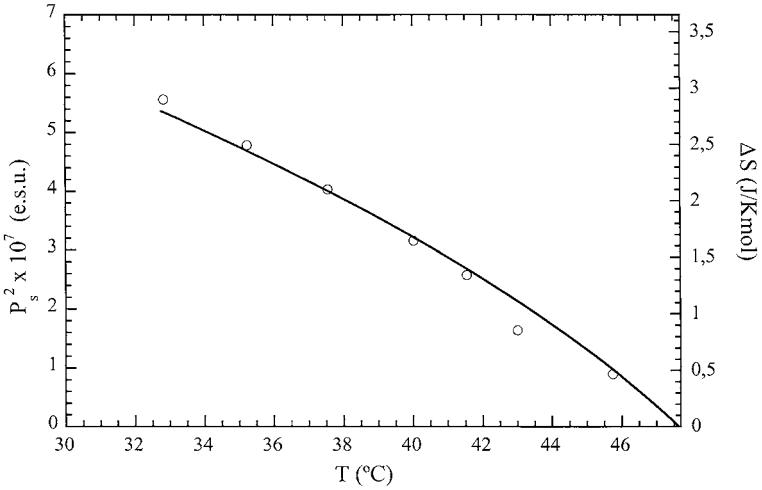

Fig. 5. Order parameter behaviour in the TGS ferro-paraelectric phase transition. The experimental phase transition entropy: $\Delta S = S_0 - S$ (continuous line) is fitted with the square of the spontaneous polarization (○) [14]. The best fit has been found, in the range $T_0 - T \leq 15$°C, for $C = 2312$ K.

heat of the phase transition can be independently calculated from

$$\Delta C_p = \left(\frac{4\pi}{C}\right)^2 \frac{T}{(4\beta^2 - (64\pi\gamma/C)(T - T_0))^{1/2}} \qquad (10)$$

An equivalent form of this equation is given by the following linear expression:

$$\left(\frac{T}{\Delta C_p}\right)^2 = \frac{4\beta^2}{(4\pi/C)^4} - \frac{16\gamma}{(4\pi/C)^3}(T - T_0) \qquad (11)$$

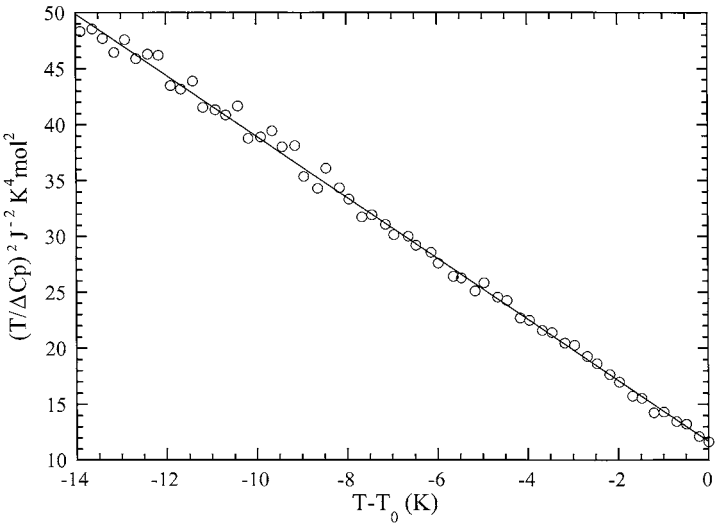

Fig. 6. Linearity of the experimental points in accordance with the Eq. (11). A least squares fit of $(T/\Delta C_p)^2$ vs. $(T - T_0)$ allowed us to obtain the values for the phenomenological coefficients β and γ by means of Eq. (11) (see Table 1).

Table 1
Phenomenological coefficient values obtained by different experimental methods

	T_0 (°C)	C (K)	β (e.s.u.)	γ (e.s.u.)	Method
Hoshino et al. [14]	48.0	3200	9.3×10^{-10}	–	P_s, ε
Ema et al. [18]	48.0	–	6.5×10^{-10}	6.6×10^{-18}	ΔC_p (ac cal.)
Tobón and Gordon [19]	48.9	3414	4.4×10^{-10}	12.0×10^{-18}	P_s, ε
Tobón and Gordon [19]	48.9	3414	4.4×10^{-10}	3.0×10^{-18}	ΔC_p (ac cal.)
This work	48.7	2312	9.6×10^{-10}	10.0×10^{-18}	ΔC_p (ac cal.)

As shown in Fig. 6, an excellent correlation between the experimental points and the fitted values is obtained.

A least squares fit of $(T/\Delta C_p)^2$ versus $(T - T_0)$ was used to calculate the values for the remaining phenomenological coefficients: $\beta = 9.64 \times 10^{-10}$ (e.s.u.) and $\gamma = 10.01 \times 10^{-18}$ (e.s.u.). In Table 1, these results are compared with some of the data found in the literature. Finally, in Fig. 7 the experimental specific heat points are plotted together with Eq. (10) using the calculated values for C, β and γ.

The observed discrepancies are commonly found in this kind of phenomenological approaches. They can be assigned to the use of different samples, but also to the experimental procedures and the selected order expansion of the free energy. For example, Tobón and Gordon [19] find different coefficient values when either the specific heat or the spontaneous polarization data are used to fit the corresponding phenomenological equations. On the other hand, the values for the Curie constant (C) are usually established from the fitting of the experimental permitivity above the transition temperature to the Curie law: $\varepsilon = C/(T - T_0)$ [14]. This law is obtained from the Landau expansion to the fourth order and if the sample polarization is assumed to be very small. As far as these experiments have to be performed under an applied AC electric field, the validity of the Curie law is restricted to the very near proximity of T_0. Nevertheless, in our case, the Curie constant is determined in the ferroelectric phase from the experimental entropy and the spontaneous polarization (Eq. (9)). Both quantities were determined at zero electric field and in a wide temperature range below T_0.

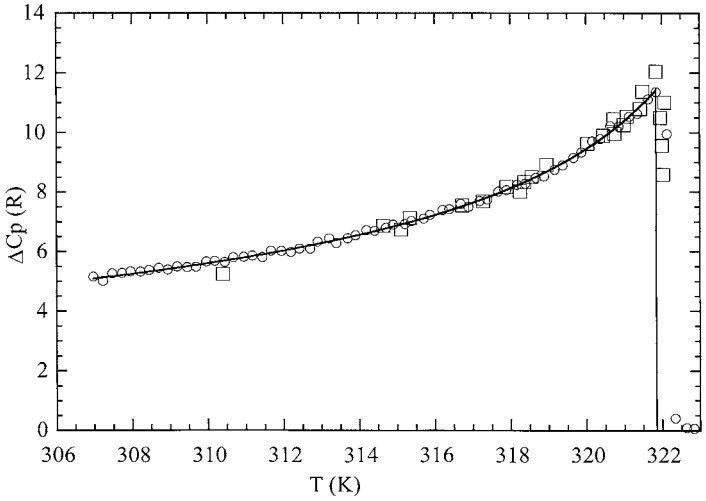

Fig. 7. The experimental C_p data (○) have been plotted together with the curve obtained by (10) with the use of the calculated phenomenological coefficients; (□) represent some of the adiabatic specific heat points from Taraskin et al. [16].

Acknowledgements

This work was supported by the Universidad del País Vasco under projects UPV 060.310-EB069/96 and UPV 060.310-G16/98.

References

[1] E.F. Westrum, G.T. Furukawa, J.P. Cullough, in: J.P. Cullough, D.W. Scott (Eds.), Experimental Thermodynamics, Butterworth, London, 1968, pp. 133–213.
[2] E. Gmelin, Thermochim. Acta 304/305 (1997) 1.
[3] I. Hatta, A. Ikushima, J. Phys. Chem. Solids 34 (1973) 57.
[4] A. Eichler, W. Gey, Rev. Sci. Instrum. 50 (11) (1979) 1445.
[5] S. Stokka, K. Fossheim, J. Phys. E: Sci. Instrum. 15 (1982) 123.
[6] C.W. Garland, Thermochim. Acta 88 (1985) 127.
[7] M. Castro, J.A. Puértolas, J. Therm. Anal. 41 (1994) 1245.
[8] G.S. Iannachione, D. Finotello, Phys. Rev. E 50 (1994) 4780.
[9] I. Hatta, H. Ichikawa, M. Todoki, Thermochim. Acta 267 (1995) 83.
[10] O.M. Corbino, Phys. Z. 11 (1910) 413.
[11] P.F. Sullivan, G. Seidel, Phys. Rev. 173 (1968) 679.
[12] P. Handler, D.E. Mapother, M. Rayl, Phys. Rev. Lett. 19 (7) (1967) 356.
[13] J.E. Graebner, Rev. Sci. Instrum. 60 (6) (1989) 1123.
[14] S. Hoshino, T. Mitsui, F. Jona, R. Pepinsky, Phys. Rev. 107 (5) (1957) 1255.
[15] R. Bachmann, F.J. DiSalvo Jr., T.H. Geballe, R.L. Greene, R.E. Howard, C.N. King, H.C. Kirsch, K.N. Lee, R.E. Schwall, H.U. Thomas, R.B. Zubeck, Rev. Sci. Instrum. 43 (2) (1972) 205.
[16] S.A. Taraskin, B.A. Strukov, V.A. Fedorikhin, N.V. Belugina, V.A. Meleshina, Sov. Phys. Solid State 19 (10) (1977) 1721.
[17] K.S. Aleksandrov, Y.N. Flerov, Sov. Phys. Solid State 21 (2) (1979) 195.
[18] K. Ema, K. Hamano, Y. Ikeda, J. Phys. Soc. Jpn. 46 (1) (1979) 345.
[19] R. Tobón, J.E. Gordon, Ferroelectrics 17 (1977) 409.